

Lepton Flavour Universality tests at Belle II

Giovanni Gaudino^{a,b,*}

^a*Scuola Superiore Meridionale,
Via Mezzocannone, 4, 8018, Napoli, Italia*

^b*INFN - Sezione di Napoli,
via Cintia, 80126, Napoli, Italia*

E-mail: gaudino@na.infn.it

We present some recent tests of lepton universality with semileptonic decays of B -mesons. The analyses are based on data collected at the $\Upsilon(4S)$ resonance by the Belle II experiment, for an integrated luminosity of 189 fb^{-1} .

This report includes two key analyses focusing on τ over μ/e lepton universality. The first is the measurement of the branching-fraction ratio $R(D_{\tau/\ell}^*) = \mathcal{B}(\bar{B} \rightarrow D^* \tau^- \bar{\nu}_e) / \mathcal{B}(\bar{B} \rightarrow D^* \ell^- \bar{\nu}_\mu)$ using hadronic tagging. The second is the first measurement of the inclusive ratio $R(X_{\tau/\ell}) = \mathcal{B}(\bar{B} \rightarrow X \tau^- \bar{\nu}_e) / \mathcal{B}(\bar{B} \rightarrow X \ell^- \bar{\nu}_\mu)$.

We also present the branching-fraction ratios $R(X_{e/\mu}) = \mathcal{B}(\bar{B} \rightarrow X e^- \bar{\nu}_e) / \mathcal{B}(\bar{B} \rightarrow X \mu^- \bar{\nu}_\mu)$ and the first measurement of a comprehensive set of five angular asymmetries using $\bar{B}^0 \rightarrow D^+ \ell^- \bar{\nu}_\ell$ decays.

All results presented are consistent with their corresponding Standard Model predictions and, where applicable, with the experimental world averages.

Workshop Italiano sulla Fisica ad Alta Intensità (WIFAI2023)

8-10 November 2023

Dipartimento di Architettura dell'Università Roma Tre, Rome, Italy

*Speaker

1. Introduction

In the Standard Model, electroweak force carriers interact with the same coupling with the charged leptons e , μ and τ , a symmetry known as lepton universality (LU). Semileptonic B -meson decays provide a very accurate test of the Standard Model, as both experimental measurements and theoretical predictions can achieve high accuracy. The latter is further enhanced by directly comparing properties like angular asymmetries or branching fractions between lepton flavors, thanks to the systematic uncertainties cancellation linked to common factors.

2. The Belle II detector, experimental data and MC simulations

The Belle II experiment, situated at the SuperKEKB collider in Tsukuba, Japan, primarily collected data at the $\Upsilon(4S)$ resonance, focusing on B meson decays. Key components of the Belle II detector include the Vertex Detector, which is composed of Pixel Detector (PXD) and a Silicon Vertex Detector (SVD) for micrometric-level vertexing and tracking below 50 MeV of transverse momentum, the Central Drift Chamber (CDC) for momentum measurements, Time-Of-Propagation (TOP) counters and ring-imaging Cherenkov counters for particle identification (ARICH), an Electromagnetic Calorimeter (ECL) for detecting electrons, photons and neutral particles, and an RPC system (KLM) for muon and K_L detection.

The dataset used for analysis in this report comprises an integrated luminosity of 189 fb^{-1} (from 2019 to 2021). Experimental results are interpreted and compared with Standard Model predictions using Monte Carlo simulations, employing software packages such as EVTGEN[9], PYTHIA[8], and KKMC[10]. The full detector responses and simulations are executed with GEANT4, while data and Monte Carlo reconstructions are performed using the Belle II analysis software framework, basf2 [11].

2.1 Full Event Interpretation: FEI

The Full Event Interpretation (FEI) [17] is an algorithm used in the Belle II experiment to categorize events into signal-side (the B decay) and tag-side (the other B produced in the event). It provides crucial details about B -decays, such as event type (e.g. $q\bar{q}$, $\tau\tau$ or $B\bar{B}$, decay vertex, and the reconstructed four-momentum of tag and signal B mesons. FEI employs Multivariate Classifiers for each decay channel and is trained on Monte Carlo data within the basf2 software package. The method, used with a hadronic tagging approach, offers high purity but limited tagging efficiency compared to semileptonic tagging, where hadronic tag means a B_{tag} decay in only hadronic particles and semileptonic means a B_{tag} decay with at least one lepton in the final state. In all the analyses presented here, the hadronic tagging method is employed.

3. Measurement of $R(D_{\tau/\ell}^*)$ with hadronic tag

The first lepton-flavour universality test presented here involves the measurement of the ratio $R(D_{\tau/\ell}^*)$ [1], defined as $\mathcal{B}(\bar{B} \rightarrow D^* \tau^- \bar{\nu}) / \mathcal{B}(\bar{B} \rightarrow D^* \ell^- \bar{\nu})$. For both the numerator and denominator, a single lepton is required in the final state to eliminate normalization effects via the ratio,

and causing the cancellation of numerous systematics, i.e. the τ is only reconstructed in the fully leptonic decays ($\tau \rightarrow \ell\nu\nu$). Leptons are identified using likelihood ratios.

Charge conjugation is implied in all physical processes, and natural units are utilized.

The hadronic component of the B decay is reconstructed through specific decay chains, suppressing combinatorial background by imposing a requirement of no other charged particles in the event. The reconstruction uses $D^* \rightarrow D^+\pi^0$ and $D^* \rightarrow D^0\pi^0$ decay chains, each with 11 sub-decay modes.

Signal extraction is accomplished through a 2D maximum-likelihood fit in E_{ECL} and M_{miss}^2 . The former represents the sum of the energy deposits in the calorimeter not associated to either B_{tag} or B_{sig} . The latter, M_{miss}^2 , is the squared magnitude of the missing 4-momentum. Fig. 4 illustrates the distributions of these variables for three different samples, the numerator of $R(D_{\tau/\ell}^*)$, the denominator and the main background $\bar{B} \rightarrow D^{**}\ell^-\nu$.

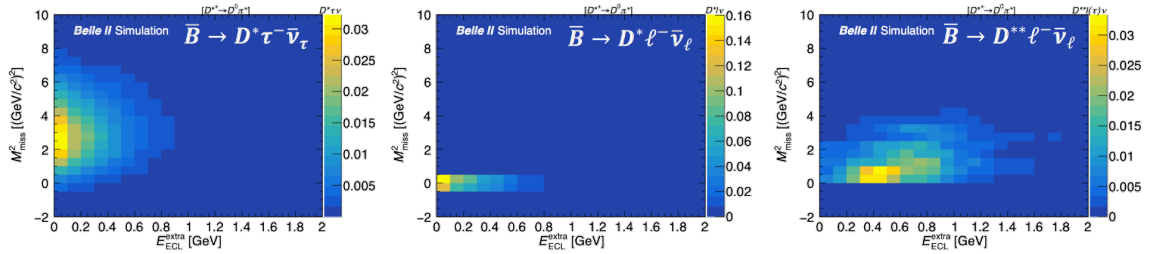


Figure 1: E_{ECL} vs M_{miss}^2 distribution of three different samples. $\bar{B} \rightarrow D^*\tau^-\nu$ is on the left plot, $\bar{B} \rightarrow D^*\ell^-\nu$ is in the center and $\bar{B} \rightarrow D^{**}\ell^-\nu$ is in the right plot.

To validate and correct shapes of the PDF used in the fit and normalizations, three control samples are employed. Background contributions from misidentified D mesons are corrected in distinct M_{miss}^2 regions, using a sideband of the $\Delta M = M_{D^*} - M_D$ variable. A correction of 15 ± 7 MeV is applied to neutral cluster energies to address an observed excess at lower values in the control region with $M_{\text{miss}}^2 < 1 \text{ GeV}^2$.

In the signal extraction fit, signal, normalization, and $\bar{B} \rightarrow D^{**}\ell^-\nu$ yields are left free, while background contributions from misidentified D mesons are constrained based on their calibration in the ΔM control region. Other backgrounds are fixed according to their predicted branching fractions. The result obtained is

$$R(D_{\tau/\ell}^*) = 0.267_{-0.039-0.033}^{+0.041+0.028}$$

The main sources of systematic uncertainty are MC statistics and the E_{ECL} shape. Our result is consistent with both the Standard Model prediction and the world average [12].

4. First Measurement of $R(X_{\tau/\ell})$ with hadronic tag

The study of the inclusive decay branching fraction ratio, denoted as $R(X_{\tau/\ell}) = \mathcal{B}(\bar{B} \rightarrow X\tau^-\bar{\nu})/\mathcal{B}(\bar{B} \rightarrow X\ell^-\bar{\nu})$ is another robust test of the Standard Model's assumption of heavy to light lepton universality. This ratio has been experimentally investigated for the first time at Belle II in [2].

Stringent lepton identification thresholds and rejection of specific hadron combinations mitigate

fake lepton contributions and suppress secondary decays in the analysis.

All remaining tracks and neutral ECL clusters are part of the hadronic system X , and its mass is denoted as M_X . Using the information on the X hadronic system, we can finally compute M_{miss}^2 .

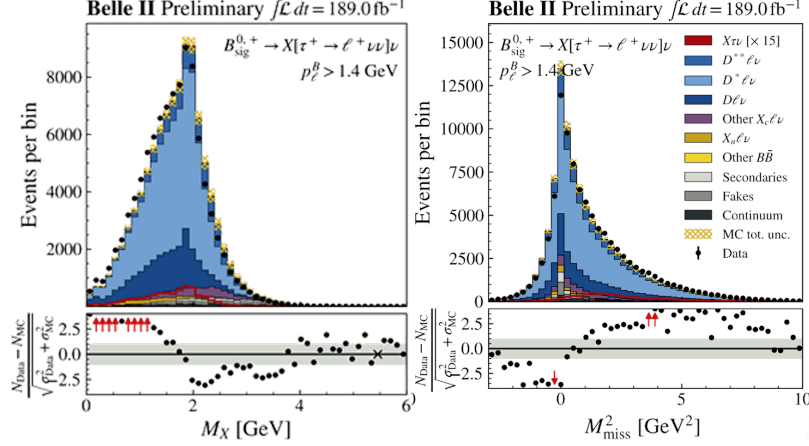


Figure 2: M_X (left) and M_{miss}^2 (right) distributions before the corrections for $D \rightarrow K_L X$ are applied.

We observe a significant excess in low M_X and a deficit in the high range as shown in Fig. 2. This is mainly due to the incorrect modeling of $D \rightarrow K_L X$ decays. The disagreement is corrected with a proper data-driven reweighting, using a high- p_ℓ control region. Secondary and fake processes are reweighted in two-dimensional intervals of p_ℓ and M_X using the same-flavor control region, where both B had the same reconstructed flavor. The signal is finally extracted using a two-dimensional binned maximum-likelihood, in bins of p_ℓ and M_X .

The results are

$$R(X_{\tau/e}) = 0.232 \pm 0.020 \pm 0.037$$

$$R(X_{\tau/\mu}) = 0.222 \pm 0.027 \pm 0.050$$

$$R(X_{\tau/\ell}) = 0.228 \pm 0.016 \pm 0.050$$

Belle II results are consistent with the SM prediction $R(X_{\tau/\ell})_{\text{SM}} = 0.223 \pm 0.005$, as derived in Refs. [14–16], and are also consistent with the world average of $R(D_{\tau/\ell}^*)$.

5. Measurement of $R(X_{e/\mu})$ with Hadronic Tag

In this analysis, presented in Ref. [3], we provide the first measurement of the inclusive ratio of branching fractions $R(X_{e/\mu})$.

The reconstruction is the same as the $R(X_{\tau/\ell})$, presented in Sec. 4. Additionally, we impose that the lepton candidate must have a momentum in the rest frame of the B_{sig}^ℓ meson $p_B^\ell > 1.3 \text{ GeV}$ to suppress most of the background coming from hadrons and secondary cascade decays.

Moreover we employ a BDT trained on event-shape quantities to suppress continuum backgrounds. Any remaining continuum events are modeled using the off-resonance data sample.

We extract the signal yields in a binned maximum-likelihood fit to the p_B^ℓ distributions of each

lepton flavor. The fit is performed simultaneously in the e and μ channels to ensure that branching-fraction and form-factor uncertainties from $\bar{B} \rightarrow X\ell^-\bar{\nu}_\ell$ are cancelled in the ratio.

$B\bar{B}$ background yields are free to vary around the yield extracted from a background-enriched control sample. To constrain continuum background yields, we utilize the collected 60 MeV below the $B\bar{B}$ threshold.

The measured value of $R(X_{e/\mu})$ is found to be

$$R(X_{e/\mu}) = 1.007 \pm 0.09 \pm 0.019.$$

Our result is consistent with the SM expectation of 1.006 ± 0.001 [16].

6. Angular asymmetries in $\bar{B}^0 \rightarrow D^+\ell^-\bar{\nu}_\ell$

We study the angular asymmetries in the decays $B^0 \rightarrow D^*\ell^-\bar{\nu}_\ell$ and their differences between electron and muon modes, utilizing five angular observables: A_{FB} , S_3 , S_5 , S_7 , and S_9 . The $B^0 \rightarrow D^*\ell^-\bar{\nu}_\ell$ decays are characterized by a recoil parameter $w \equiv (m_{B^0}^2 + m_{D^*}^2 - (p_{B^0} - p_{D^*})^2)/(2m_{B^0}m_{D^*})$, along with three helicity angles defined in Fig. 3. The analysis is reported in Ref.[4].

The angular variables are defined as:

$$A_x(w) = \left(\frac{d\Gamma}{dw}\right)^{-1} \int_{-1}^1 \text{sgn}(x) \frac{d^2\Gamma}{dw dx} dx$$

where $x = \cos \theta_\ell$ for A_{FB} , $\cos 2\chi$ for S_3 , $\cos \chi \cos \theta_V$ for S_5 , $\cos \theta_V \sin \chi$ for S_7 and $\sin 2\chi$ for S_9 . The difference of the A_x between the muon and electron channel is called ΔA_x . The reconstruction of the decay is the same of the one in the $R(D_{\tau/\ell}^*)$ explained in Sec. 3. We perform a binned maximum-likelihood template fit to the M_{miss}^2 distributions to extract signal yields. The extracted yields undergo corrections for migration between bins due to the experimental resolution. To enhance sensitivity to SM extensions, we determine all asymmetry variables for both electron and muon modes in three different w ranges: [1.000, 1.503] (full range), [1.000, 1.275] (low range), and [1.275, 1.503] (high range).

The results are summarized in Figure 3. The χ^2 tests conducted in each of the three w regions exhibit strong conformity with the predictions of the Standard Model. The minimum p -value obtained is 0.13, indicating no significant deviation from expectations, and thus, no evidence supporting LUV is detected. The primary source of systematic uncertainty stems from the size of the simulation sample used to estimate the migration matrix, contributing approximately 25% to 50% of the statistical uncertainties. Other systematic uncertainties, such as lepton identification, remain minimal, typically below 0.004.

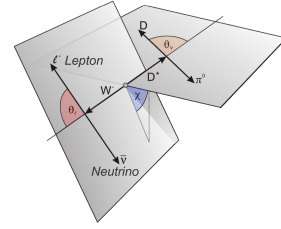


Figure 3: Schematic representation of a $B \rightarrow D^*\ell\nu$ decay

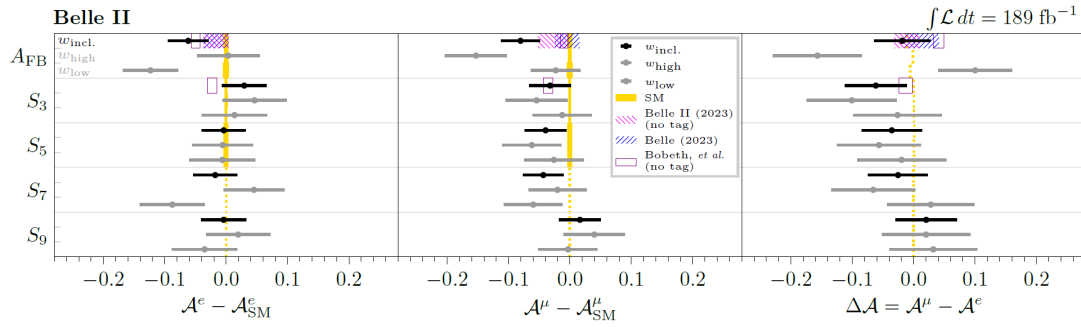


Figure 4: Measured asymmetries for electron (left) and muon (middle) modes, along with their differences (right). Black and grey points represent different w ranges, reported in the text. The yellow solid boxes or dashed lines represent the Standard Model (SM) predictions

References

- [1] I. Adachi *et al.* [Belle-II], *A test of lepton flavor universality with a measurement of $R(D^*)$ using hadronic B tagging at the Belle II experiment*, [arXiv:2401.02840 \[hep-ex\]](https://arxiv.org/abs/2401.02840).
- [2] I. Adachi *et al.* [Belle-II], *First measurement of $R(X_{\tau/\ell})$ as an inclusive test of the $b \rightarrow c\tau\nu$ anomaly*, [arXiv:2311.07248 \[hep-ex\]](https://arxiv.org/abs/2311.07248).
- [3] L. Aggarwal *et al.* [Belle-II], *Test of Light-Lepton Universality in the Rates of Inclusive Semileptonic B -Meson Decays at Belle II*, *Phys. Rev. Lett.* **131** (2023) no.5, 051804, [doi:10.1103/PhysRevLett.131.051804](https://doi.org/10.1103/PhysRevLett.131.051804), [arXiv:2301.08266 \[hep-ex\]](https://arxiv.org/abs/2301.08266).
- [4] I. Adachi *et al.* [Belle-II], *Tests of Light-Lepton Universality in Angular Asymmetries of $B^0 \rightarrow D^* - \ell\nu$ Decays*, *Phys. Rev. Lett.* **131** (2023) no.18, 181801, [doi:10.1103/PhysRevLett.131.181801](https://doi.org/10.1103/PhysRevLett.131.181801), [arXiv:2308.02023 \[hep-ex\]](https://arxiv.org/abs/2308.02023).
- [5] K. Akai *et al.* [SuperKEKB], *SuperKEKB Collider*, *Nucl. Instrum. Meth. A* **907** (2018), 188-199, [doi:10.1016/j.nima.2018.08.017](https://doi.org/10.1016/j.nima.2018.08.017), [arXiv:1809.01958 \[physics.acc-ph\]](https://arxiv.org/abs/1809.01958).
- [6] E. Kou *et al.* [Belle-II], *The Belle II Physics Book*, *PTEP* **2019** (2019) no.12, 123C01, [doi:10.1093/ptep/ptz106](https://doi.org/10.1093/ptep/ptz106), [arXiv:1808.10567 \[hep-ex\]](https://arxiv.org/abs/1808.10567).
- [7] T. Abe *et al.* [Belle-II], *Belle II Technical Design Report*, [arXiv:1011.0352 \[physics.ins-det\]](https://arxiv.org/abs/1011.0352).
- [8] T. Sjöstrand *et al.*, *An introduction to PYTHIA 8.2*, *Comput. Phys. Commun.* **191** (2015), 159-177, [doi:10.1016/j.cpc.2015.01.024](https://doi.org/10.1016/j.cpc.2015.01.024), [arXiv:1410.3012 \[hep-ph\]](https://arxiv.org/abs/1410.3012).
- [9] D. J. Lange, *The EvtGen particle decay simulation package*, *Nucl. Instrum. Meth. A* **462** (2001), 152-155, [doi:10.1016/S0168-9002\(01\)00089-4](https://doi.org/10.1016/S0168-9002(01)00089-4).
- [10] S. Jadach, B. F. L. Ward and Z. Was, *The Precision Monte Carlo event generator KK for two fermion final states in e^+e^- collisions*, *Comput. Phys. Commun.* **130** (2000), 260-325, [doi:10.1016/S0010-4655\(00\)00048-5](https://doi.org/10.1016/S0010-4655(00)00048-5), [arXiv:hep-ph/9912214 \[hep-ph\]](https://arxiv.org/abs/hep-ph/9912214).

- [11] T. Kuhr *et al.* [Belle-II Framework Software Group], *The Belle II Core Software*, *Comput. Softw. Big Sci.* **3** (2019) no.1, 1, doi:[10.1007/s41781-018-0017-9](https://doi.org/10.1007/s41781-018-0017-9), arXiv:[1809.04299](https://arxiv.org/abs/1809.04299) [physics.comp-ph].
- [12] Y. S. Amhis *et al.* [HFLAV], *Phys. Rev. D* **107** (2023) no.5, 052008 doi:[10.1103/PhysRevD.107.052008](https://doi.org/10.1103/PhysRevD.107.052008) [arXiv:[2206.07501](https://arxiv.org/abs/2206.07501) [hep-ex]].
- [13] M. Rahimi and K. K. Vos, *JHEP* **11** (2022), 007 doi:[10.1007/JHEP11\(2022\)007](https://doi.org/10.1007/JHEP11(2022)007) [arXiv:[2207.03432](https://arxiv.org/abs/2207.03432) [hep-ph]].
- [14] M. Freytsis, Z. Ligeti and J. T. Ruderman, *Phys. Rev. D* **92** (2015) no.5, 054018 doi:[10.1103/PhysRevD.92.054018](https://doi.org/10.1103/PhysRevD.92.054018) [arXiv:[1506.08896](https://arxiv.org/abs/1506.08896) [hep-ph]].
- [15] Z. Ligeti, M. Luke and F. J. Tackmann, *Phys. Rev. D* **105** (2022) no.7, 073009 doi:[10.1103/PhysRevD.105.073009](https://doi.org/10.1103/PhysRevD.105.073009) [arXiv:[2112.07685](https://arxiv.org/abs/2112.07685) [hep-ph]].
- [16] M. Rahimi and K. K. Vos, *JHEP* **11** (2022), 007 doi:[10.1007/JHEP11\(2022\)007](https://doi.org/10.1007/JHEP11(2022)007) [arXiv:[2207.03432](https://arxiv.org/abs/2207.03432) [hep-ph]].
- [17] T. Keck, F. Abudinén, F. U. Bernlochner, R. Cheaib, S. Cunliffe, M. Feindt, T. Ferber, M. Gelb, J. Gemmler and P. Goldenzweig, *et al.* *Comput. Softw. Big Sci.* **3** (2019) no.1, 6 doi:[10.1007/s41781-019-0021-8](https://doi.org/10.1007/s41781-019-0021-8) [arXiv:[1807.08680](https://arxiv.org/abs/1807.08680) [hep-ex]].